Vacuum 187 (2021) 110105

Contents lists available at ScienceDirect

Vacuum

journal homepage: http://www.elsevier.com/locate/vacuum

Regularities of PLA mechanical property modification under ion implantation conditions

I.V. Vasenina [a,*], O.A. Laput [b], I.A. Kurzina [b]

[a] P.N. Lebedev Physical Institute, 53, Leninsky Prospect, Moscow, 119333, Russia
[b] National Research Tomsk State University, 36 Lenin Ave, Tomsk, 634050, Russia

ARTICLE INFO

Keywords:
Polylactic acid
Ion implantation
Projected ion range
Mechanical characteristics
Microhardness
Long-range effect

ABSTRACT

The investigations of the surface physicochemical properties of polylactic acid (PLA) modified by argon, carbon and silver ion implantation to fluences of $1\cdot10^{14}$, $1\cdot10^{15}$ and $1\cdot10^{16}$ cm^{-2} and energies of 20 keV, 20 keV and 42 keV respectively are described. The projected ion ranges in the polymer matrix are estimated by the computer simulation with the TRIDYN code, as well as energies of electron and nuclear stopping are assessed according to the SRIM modelling. The microhardness and elastic modulus are established to be dependent on the degree of crystallinity of the material. It was found that the microdistortions and strains of the PLA crystal lattice increase after ion implantation due to the structural alteration and defect formation. Long-range effect expressed as bigger depth of modified surface layer than the ion range in the material is suggested as a result of the radiation-stimulated diffusion and thermal restructuring of the material.

1. Introduction

Polylactic acid is a biodegradable polymer used in biomedicine as wound healing bandage, membrane systems, fasteners, surgical sutures, and pins. This material is of great interest for study, in particular, after modification by various methods of surface treatment. In our early works, we have presented the results of the polylactic acid surface property investigation after treatment with ion [1–3] and electrons [4] beams, as well as with plasma flows [5]. Some polymer properties such as wettability and surface energy are described in details [6,7], but the mechanical characteristics such as microhardness and elastic modulus are insufficiently studied. Mechanical properties of polymers are important factors for their practical application. It is known that the increase of amorphous regions in polycrystalline polymers promotes the degradation rate of the implants in cellular medium [8].

Measurement of microhardness is one of the most easily and quickly implemented methods of mechanical testing, which help to control the product characteristics and study structural transformations. In addition, it can be used to indirectly assess other mechanical characteristics in the presence of appropriate correlations. Mechanical properties are also functionally important, and understanding the patterns of their change under surface treatment conditions is necessary to further expand the possibilities of the practical application of this material. In addition, it is important to understand what effect changes in the surface layer structure have on these properties.

The aim of this work is to identify the regularities of modification of physical and mechanical characteristics and their relationship with structural changes in the polylactic acid surface layer under conditions of ion-beam treatment.

2. Materials and methods

2.1. Preparation of PLA samples

Synthesis of the polylactic acid ($[\text{-OCH}(CH_3)\text{-CO-}]_n$) was carried out according to the procedure [9], where L-lactide was used as the initial monomer. The experimental samples were prepared from the 7% solution of polylactic acid (MW = 250 000 g/mol) in chloroform dried at room temperature in a Petri dish. The size of PLA samples was 10 × 10 mm^2, the thickness is ~1 mm.

2.2. Ion implantation

Implantation of Ag, Ar and C ions was carried out using MEVVA-V. Ru vacuum arc ion source [10] to fluences of $1\cdot10^{14}$, $1\cdot10^{15}$, and $1\cdot10^{16}$ cm^{-2} at the accelerating voltage of 20 kV. Charge state

* Corresponding author.
E-mail address: ivpuhova@mail.ru (I.V. Vasenina).

https://doi.org/10.1016/j.vacuum.2021.110105
Received 19 November 2020; Received in revised form 26 January 2021; Accepted 26 January 2021
Available online 4 February 2021

Table 1
Distribution of ion charge state Q in the beam of vacuum arc discharge.

Element	Atomic number Z	Q = 1+	2+	3+	4+	Q_p	U_{acc}, kV	<E_0>, keV
Ag	47	13%	61%	25%	1%	2.1	20	42
Ar	18	100%				1	20	20
C	6	100%				1	20	20

distributions of the ion beams were measured by a time-of-flight mass-to-charge spectrometer [11,12]. Argon and carbon ions were singly ionized (Ar^+, C^+); therefore their energy was 20 keV. Silver ion beam contains ions with 1+, 2+, 3+, 4+ charge states; since we consider the mean charge state of the extracted beam is 2.1+ ($Ag^{<2.1+>}$), the average energy of silver ions was 42 keV. The PLA samples were mounted on a water-cooled target holder and the temperature of them during the experiments was keep at 20 °C. A working pressure of $1 \cdot 10^{-6}$ Torr was maintained by an oil-free high-vacuum cryogenic pump. Current density of ions in the place of sample location was 3 mA cm^{-2} at the pulse duration of 250 μs and pulse frequency of 0.1 s^{-1}. In this case, the ion flux density was $2 \cdot 10^{11}$ $cm^{-2}s^{-1}$. For silver and carbon generation a vacuum arc discharge with cathodes from the corresponding materials was used. The working pressure in this case was $1 \cdot 10^{-6}$ Torr. Argon ions were extracted from the plasma of glow discharge with the hollow cathode. For its functioning, the ion source discharge system was filled with the corresponding gas (argon). The working pressure in the area of the experimental sample location was $2 \cdot 10^{-4}$ Torr.

2.3. Characterization techniques

Depth ion distributions were calculated by the projected range simulation in a polymer matrix by the TRIDYN code [13], based on the mathematical modelling of the ion transition in a substance by the Monte Carlo method [14]. In addition, SRIM-2013.00 modelling was used for the calculations of electron and nuclear mass stopping power [15].

Ions in the beam have different charge states; their energy E_0 changes depending on them. Hence, the whole ion flow should be divided on parts according to the charge states and percentage of ions in each charge state (Table 1).

The average energy in the ion beam:

$$< E_0 > = U_{acc} \cdot Q_p, \quad (1)$$

where Q_p – mean charge state for the average energy calculation in the ion beam, U_{acc} – accelerating voltage, kV.

The stresses of the PLA crystal lattice were determined from the X-ray diffraction (XRD) patterns from Ref. [1] using the half-width of the main lines. Plotting the dependence $\frac{\beta \cdot \cos\theta}{\lambda} = f(\frac{4 \cdot \sin\theta}{\lambda})$ for the main lines allows us to determine microdistortions of the crystal structure. The relative error of interplanar distance <$\Delta d/d$> was determined according to the straight-line slope for the main PLA lines [16]:

$$< \Delta d/d > = \mathrm{ctg}\cdot\theta \cdot \Delta\theta \quad (2)$$

Stresses σ in the material was calculated taking into account Young's modulus E [16]:

$$\sigma = < \Delta d/d > E \quad (3)$$

Nanotest 600 hardness testing instrument was used for microhardness of PLA samples measurements. With using Berkovich tip (truncated trihedral diamond pyramid, apex angle is 142°) with a varying load of 0.5; 1; 2; 3 mN, the indenter penetration depth reached 1200 nm.

3. Results

3.1. Ranges of Ag, Ar, C ions in polylactic acid

The ion range in a surface layer is an important characteristic of the ion-implanted materials, which determines the depth and area of propagation of the ion treatment effects. The projected ion ranges in the PLA surface layer obtained by the TRIDYN code are presented in Table 2. The silver ion beam consists of the ions with different charge states (1+, 2+, 3+, 4+), and, accordingly, with different energies (20; 40; 60; 80 keV) (Table 1). Thus, the projected Ag ion ranges in the PLA surface layer are 57.5; 87.5; 117.5; 122.5 nm for four ion charge states respectively at the fluence of $1 \cdot 10^{16}$ cm^{-2}. The total calculated penetration depth of silver ions with the average charge state of <2.1+> and the energy of 42 keV $Ag^{<2.1+>}$ into the PLA is 82.5 nm (Fig. 1, a). It was shown that argon ions can penetrate in the PLA surface layer depth up to 87.5 nm at the fluence of $1 \cdot 10^{16}$ cm^{-2} with depth of the maximum Ar^+ concentration ≈37.5 nm, and the carbon ions C^+ – up to 176 nm with the maximum of 97.5 nm (Fig. 1b and c).

It was found that the light ions deeper penetrate into the bulk of the material, while the heavy ions are deposited on the top-surface [17]. Carbon ions have the greatest value of the ion path since carbon atomic number Z is 6 and it has the smallest atomic mass among the investigated substances (Table 2). Silver ions penetrate deeper than Ar ions despite their higher atomic mass, since the silver beam contains ions of three charge states: Ag^{1+}, Ag^{2+} and Ag^{3+}. Hence, the average energy in silver ion beam at the average charge state $Ag^{<2.1+>}$ is higher than the initial energy of carbon and argon ions. Most of the silver ions have initial energy more than 20 keV; therefore their energy is higher than that for Ag^{1+} ions. Ions with a charge of 3+ and 4+ have the highest energy and minimum mass; therefore, they penetrate deeper into the surface of the material. Thus, the mass of silver ions with charge state 2+ and higher become comparable with the mass of Ar ions, consequently, their ranges are in the almost similar values (82.5 nm for Ag ions and 87.5 nm for Ar ions).

Using the SRIM software [18] the electron $S_e = dE_e/dx$ and nuclear $S_n = dE_n/dx$ mass stopping power in the matrix surface at the Ag, Ar, C

Table 2
Projected ion range in polylactic acid calculated by TRIDYN code [8] and electron and nuclear mass stopping power according to SRIM modeling [15].

Ions	Depth of the maximum ion concentration, nm				Maximum depth of ion penetration, nm	Electron mass stopping power, dE_e/dx, keV/(μg·cm^{-2})	Nuclear mass stopping power, dE_n/dx, keV/(μg·cm^{-2})
	Ion charge state/energy						
	1+ 20 keV	2+ 40 keV	3+ 60 keV	4+ 80 keV			
Ag	32.5	47.5	67.5	72.5	82.5	1.320	9.322
Ar	37.5				87.5	1.052	3.828
C	97.5				176.0	0.914	0.635

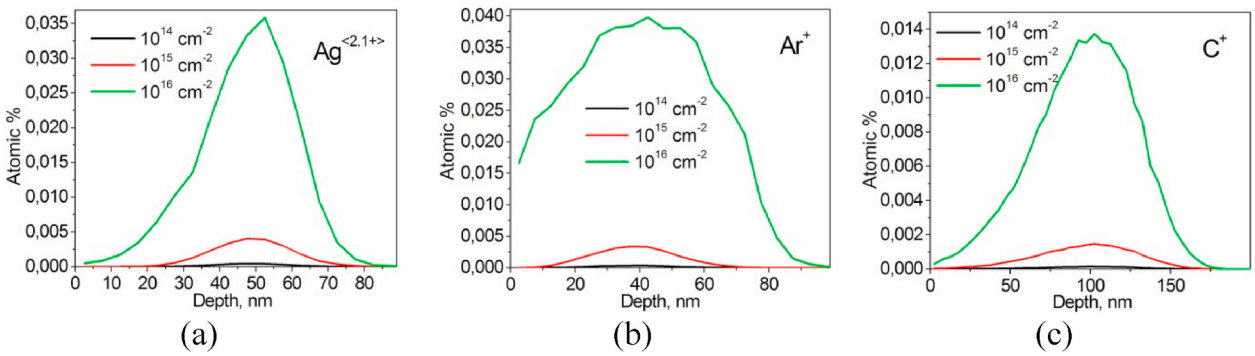

Fig. 1. Projected ion range in PLA calculated by TRIDYN code: a) silver, b) argon, c) carbon.

Table 3
Microdistortions and strains of the PLA crystal lattice.

Sample	Microdistortions of the crystal lattice, $\Delta d/d \cdot 10^{-3}$	Strains of the crystal lattice, σ, MPa
PLA initial	2.58	24.460
PLA + Ag $1 \cdot 10^{14}$ cm^{-2}	4.76	39.841
PLA + Ag $1 \cdot 10^{15}$ cm^{-2}	4.62	24.965
PLA + Ag $1 \cdot 10^{16}$ cm^{-2}	13.57	101.405
PLA + Ar $1 \cdot 10^{14}$ cm^{-2}	21.82	199.034
PLA + Ar $1 \cdot 10^{15}$ cm^{-2}	11.23	82.096
PLA + Ar $1 \cdot 10^{16}$ cm^{-2}	20.36	151.478
PLA + C $1 \cdot 10^{14}$ cm^{-2}	20.58	170.608
PLA + C $1 \cdot 10^{15}$ cm^{-2}	21.98	187.726
PLA + C $1 \cdot 10^{16}$ cm^{-2}	23.15	212.998

ion bombardment were found (Table 2). The total ion range with the initial energy E_0 is described by the formula [19]:

$$R = \int_0^{E_0} \frac{dE}{S_n + S_e}. \quad (4)$$

It was shown from Table 2 that transfer of energy from implanted silver and argon ions occurs predominantly due to nuclear collisions, and when carbon ions implanted due to electronic excitations. This is due to the fact that carbon ions have a low atomic mass and, accordingly, their velocity is higher than other ions at the same accelerating voltage. On the contrary, silver ions have the highest atomic mass, and the difference between the electron and nuclear mass stopping powers is large for them. Thus, during the implantation of silver and argon due to nuclear collisions and the formation of a region with a high density of defects, the processes of the polymer chain scission and the formation of low-molecular-weight fragments and radicals prevail. Electronic interactions lead to the excitation and ionization of molecules. The energy transfer from the interaction place leads to the excitation of neighboring parts of the polymer chain and the formation of displacement cascades (the so-called penambres, with a characteristic size of the order of 100–1000 nm) [17]. Moreover, heavy Ag ion transfers its energy mostly to target atoms thus forming recoils in collision cascade. However, recoil atoms are much lighter (C, O, H) and also interact with electrons in the target. Thus, amount of energy deposited into electronic subsystem is influenced by recoils.

3.2. The correlation of the surface layer structure modification in the ion implantation conditions and mechanical properties of polylactic acid

The change in the surface structure after ion implantation affects the mechanical properties (microhardness, elastic modulus) of polymers, which also depend on the thickness of the polymer modified layer, the parameters and methods of treatment. Polymers with a low etching rate and a high degree of crosslinking are characterized by an increase in strength and elastic modulus due to surface carbonization. The mechanical properties of materials with a high etching rate and a tendency to depolymerization (bond breaking) do not change significantly [20]. Polylactic acid, due to its heterochain structure, belongs to the type of polymers with predisposition to destruction and rupture of macromolecules upon irradiation with ion beams.

Crystallographic parameters (coherent scattering region and degree of crystallinity) as well as mechanical characteristics (microhardness and elastic modulus) of polylactic acid were established in our previous work [1]. It was found that degree of crystallinity decreases and affects the mechanical characteristics of the material. According to the obtained in Ref. [1] results, here we consider influence of ion-beam surface treatment on the internal microdistortions and strains of the PLA crystal

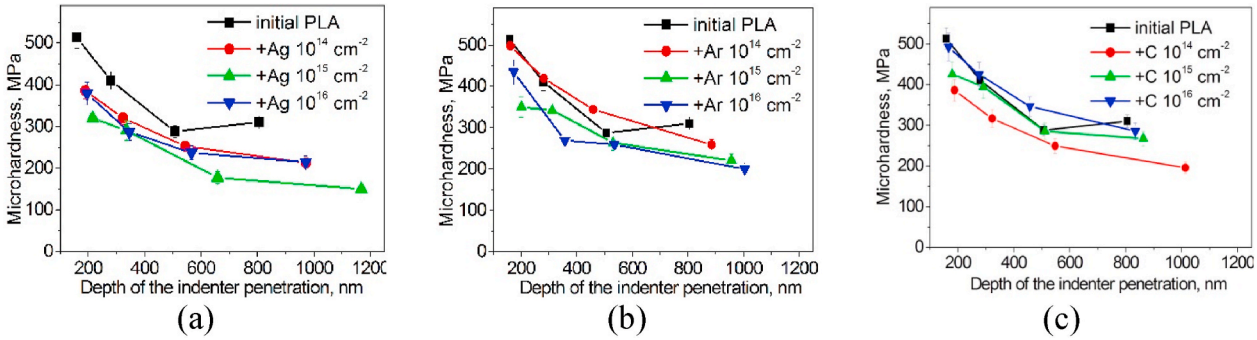

Fig. 2. Microhardness along the depth of the PLA surface layer after implantation with a) silver, b) argon, c) carbon ions.

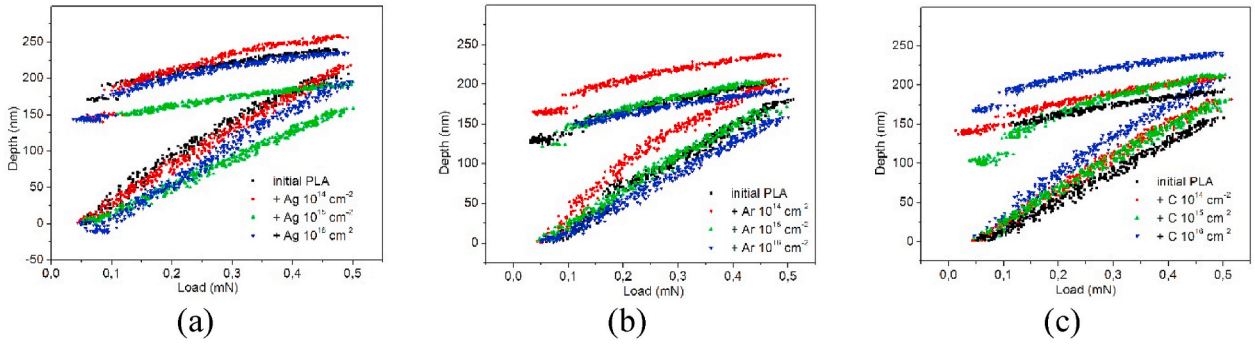

Fig. 3. Load-displacement curves at the lowest indentation loads (0 ÷ 0.5 mN) for PLA after implantation with a) silver, b) argon, c) carbon ions.

lattice (Table 3).

The polymer crystal lattice microdistortions and strains increase when the processing time and, accordingly, the radiation fluence increase, which results in other parameters and properties in the PLA surface layer alteration. Namely, the PLA microhardness and elastic modulus decrease by the factor of 1.4 and 1.75 respectively [1]. Under the ion-beam treatment conditions of the polymer, there are processes, such as ion penetration, polymer bond rupture, polymer atom displacement cascade initiation, radical formation, crosslinking of macromolecules, etc., leading to the defect formation and the PLA surface layer structure change.

The graph of the PLA microhardness change over the depth of the surface layer with change in the load on the indenter (0.5; 1; 2; 3 mN) before and after ion implantation is shown in Fig. 2. It was found that the microhardness of the initial PLA sample decreases to 40% at a depth of ~800 nm. After ion-beam treatment, the PLA microhardness decreases with increase of the load on the indenter, while the penetration depth of the indenter increases in comparison with the initial sample. This effect can be explained by the PLA surface softening during the indenter penetration [21].

It should be noted that at the $1 \cdot 10^{14}$ and $1 \cdot 10^{15}$ cm^{-2} Ag and Ar ion irradiation, the microhardness decreases, and then, with the fluence increase to $1 \cdot 10^{16}$ cm^{-2}, it increases (Fig. 2a and b). Probably, the fluence of $1 \cdot 10^{16}$ cm^{-2} is the threshold fluence for the impurity accumulation in the surface layer and the strengthening carbonized phase formation. This effect is also characteristic when carbon ion irradiation (Fig. 2, c), however, the threshold fluence in this case is $1 \cdot 10^{15}$ cm^{-2}, since at this fluence the microhardness of the PLA increases. The minimum microhardness (150 MPa) is characterized to the $1 \cdot 10^{15}$ cm^{-2} Ag-implanted PLA sample at a depth of 1170 nm (Fig. 2, a).

Fig. 3 represents the load-displacement curves at the lowest indentation loads (up to 0.5 mN). As it can be seen from Fig. 3, at the maximum load (0.5 mN) the material undergoes the plastic deformation due to its plasticity, but it recovers due to elasticity and temperature effect when unload. First, at the depth of the indenter penetration growing the PLA become softer, then the hardness returns to the original values with the reduction of the depth of the indenter penetration.

It should be noted that the projective range of ions in polylactic acid does not exceed 100 nm, and the depth of the modifying effect of ion-beam surface treatment on the mechanical properties of the PLA reaches 1200 nm. Therefore, under the ion implantation conditions, a long-range effect occurs due to radiation-induced diffusion and thermal restructuring of the material [22,23]. Also, the changes in the degree of crystallinity of the PLA surface layer testify in favor of the long-range effect, since the diffraction patterns for polymers were taken in grazing incidence diffraction regime with the grazing angle of 3° [1], the investigated depth in this case was up to ~1 μm [24], which is bigger than the projected range. Hence, we concluded that structural alterations occur deeper than ions stop and long-range effect take place.

4. Conclusions

A detailed study of the dependence of the polylactic acid structure and mechanical characteristic changes after ion implantation has been carried out. The relationship between the decrease of the mechanical characteristics and the degree of crystallinity of the PLA has been established: with increase of amorphous regions, the values of microhardness and elastic modulus decrease. As a result of intense thermal action in the track of ions, as well as radiation-stimulated diffusion, polymer macromolecules can vibrate relative to their initial state that leads to their conformation change, distortions of the crystal lattice, and the defectiveness of the material increasing. Due to the rupture of some bonds, the proportion of regions with ordered arrangement of macromolecules decreases. This phenomenon affects the mechanical characteristics of the material: decrease in the degree of crystallinity leads to the microhardness (the ability of the material to resist the penetration of the indenter) and the elastic modulus (the ability of the material to return to its original state when removed load) reduction.

It is shown that the energetic exposure on the PLA surface with Ag, Ar, C ion beams results in the microdistortions and strains of the PLA crystal lattice increase when the treatment condition changing. It was found that the effect of PLA surface modification extends much deeper than the projective ion range in the material – up to 1 μm, which is recorded by measuring the microhardness at a varying load up to 50% of the microhardness values for the initial material at the same depth as well as the degree of crystallinity alterations measured in the grazing angle mode. Consequently, structural changes and mechanical property modification under the ion implantation conditions exceed the ion penetration depth value that is why long range effect takes place.

Declaration of competing interest

The authors declare that they have no known competing financial interests or personal relationships that could have appeared to influence the work reported in this paper.

Acknowledgments

This work was supported by the Tomsk State University competitiveness improvement program. The reported study was funded by RFBR, project number 20-32-90175. Special thanks are extended to the Laboratory of Thin Films of Institute of Physics of University of São Paulo and personally to K.P. Savkin and K.V. Oskomov for assistance and support.

References

[1] I.A. Kurzina, O.A. Laput, D.A. Zuza, I.V. Vasenina, M.C. Salvadori, K.P. Savkin, D. N. Lytkina, V.V. Botvin, M.P. Kalashnikov, Surface property modification of biocompatible material based on polylactic acid by ion implantation, Surf. Coating. Technol. 388 (1–8) (2020) 125529, https://doi.org/10.1016/j.surfcoat.2020.125529.

[2] O.A. Laput, D.A. Zuza, I.V. Vasenina, K.P. Savkin, I.A. Kurzina, Effect of silver ion implantation on surface physicochemical properties of composite materials based on polylactic acid and hydroxyapatite, Vacuum 175 (1–10) (2020) 109251, https://doi.org/10.1016/j.vacuum.2020.109251.
[3] I.V. Vasenina, K.P. Savkin, O.A. Laput, D.A. Zuza, I.A. Kurzina, Surface property modification of polylactic acid by ion implantation, Preprints (2017), 2017110125, https://doi.org/10.20944/preprints201711.0125.v1.
[4] I.V. Pukhova, K.P. Savkin, O.A. Laput, D.N. Lytkina, V.V. Botvin, A.V. Medovnik, I. A. Kurzina, Effect of ion-plasma and electron-beam treatment on surface physicochemical properties of polylactic acid, Appl. Surf. Sci. 422 (2017) 856–862, https://doi.org/10.31554/978-5-7925-0524-7-2018-178-184.
[5] O.A. Laput, I.V. Vasenina, M.C. Salvadori, K.P. Savkin, D.A. Zuza, I.A. Kurzina, Low-temperature plasma treatment of polylactic acid and PLA/HA composite material, J. Mater. Sci. 54 (2019) 11726–11738, https://doi.org/10.1007/s10853-019-03693-4.
[6] A.Y. Song, Y.A. Oh, S.H. Roh, J.H. Kim, S.C. Min, Cold oxygen plasma treatments for the improvement of the physicochemical and biodegradable properties of polylactic acid films for food packaging, J. Food Sci. 81 (1) (2016) 86–96, https://doi.org/10.1111/1750-3841.13172.
[7] Y. Zhao, A. Fina, A. Venturello, F. Geobaldo, Effects of gas atmospheres on poly (lactic acid) film in acrylic acid plasma treatment, Appl. Surf. Sci. 283 (2013) 181–187, https://doi.org/10.1016/j.apsusc.2013.06.078.
[8] F.J. Balta Calleja, Microhardness relating to crystalline polymers, in: Characterization of Polymers in the Solid State I: Part A: NMR and Other Spectroscopic Methods Part B: Mechanical Methods, Advances in Polymer Science, vol. 66, 1985, pp. 118–148, https://doi.org/10.1007/3-540-13779-3_19.
[9] I.A. Kurzina, I.V. Pukhova, V.V. Botvin, D.V. Davydova, K.P. Savkin, K.V. Oskomov, E.M. Oks, New Materials Based on Polylactide Modified with Silver and Carbon Ions, Proceedings of the 5th International Scientific Conference «New Operational Technologies», Tomsk, Russia, 29-30 September 2015, AIP Conf. Proc., 1688, 2015, 030033, https://doi.org/10.1063/1.4936028.
[10] A.G. Nikolaev, E.M. Oks, K.P. Savkin, G.Yu Yushkov, I.G. Brown, Upgraded vacuum arc ion source for metal ion implantation, Rev. Sci. Instrum. 83 (2012) 2, https://doi.org/10.1063/1.3655529, 02A501.
[11] I.G. Brown, The Physics and Technology of Ion Sources, second ed., John Wiley and Sons, New York, 2004.
[12] V.I. Gushenets, A.G. Nikolaev, E.M. Oks, L.G. Vintizenko, G.Yu Yushkov, Simple and inexpensive time-of-flight charge-to-mass analyzer for ion beam source characterization, Rev. Sci. Instrum. 77 (2006), 063301, https://doi.org/10.1063/1.2206778.
[13] W. Möller, W. Eckstein, Tridyn — a TRIM simulation code including dynamic composition changes, Nucl. Instrum. Methods Phys. Res. Sect. B Beam Interact. Mater. Atoms 2 (1984) 814–818, https://doi.org/10.1016/0168-583X(84)90321-5.
[14] W. Möller, W. Eckstein, Tridyn - binary collision simulation of atomic collisions and dynamic composition changes in solids, Comput. Phys. Commun. 51 (1988) 355–368, https://doi.org/10.1016/0010-4655(88)90148-8.
[15] Interactions of ions with matter, Available online: www.SRIM.org. (Accessed 22 October 2020).
[16] A. Taylor, X-ray Metallography, John Wiley and Sons, New York, 1961.
[17] V.B. Odzhaev, I.P. Kozlov, V.N. Popok, D.V. Sviridov, Ion Implantation of Polymers, Belarusian State University, Minsk, Belarus, 1998, 197 p. (In Russian).
[18] J.F. Ziegler, M.D. Ziegler, J.P. Biersack, The stopping and range of ions in mater, Nucl. Instrum. Methods Phys. Res. Sect. B Beam Interact. Mater. Atoms 268 (2010) 1818–1823, https://doi.org/10.1016/j.nimb.2010.02.091.
[19] J. Lindhard, M. Scharff, H. Schiott, Range concepts and heavy ion ranges. (Notes on atomic collisions, II.), Mat. Fys. Medd. Dan. Vid. Selsk 33 (1963) 1–42.
[20] A. Kondyurin, M. Bilek, Ion Beam Treatment of Polymers, Application Aspects from Medicine to Space, second ed., Elsevier Ltd., Amsterdam, 2014.
[21] N.A. Palistrant, V.V. Bivol, S.V. Robu, P.S. Smertenko, The mechanism of deformation of new perspective polymer composites based on 4-aminostirole at high local voltages//Fizika i tekhnika vysokikh davlenii, Phys. Technics of High Press. 16 (2006) 153–158 (In Russian).
[22] A.Ya Bomba, B.B. Kolupaev, E.V. Lebedev, A.M. Rogalya, Study of radiation-stimulated diffusion in filled polyvinyl chloride. Elektronnaya obrabotka materialov, Electr. Treatment Mater. 41 (2005) 59–63 (In Russian).
[23] V.A. Stepanov, Radiation-stimulated diffusion in solids//Zhurnal technicheskoy fiziki, Techn. Phys. J. 68 (1998) 67–72 (In Russian).
[24] Yu P. Mironov, L.L. Meisner, A.I. Lotkov, The structure of titanium nickelide surface layers formed by pulsed electron-beam melting, Tech. Phys. 53 (2008) 934–942, https://doi.org/10.1134/S1063784208070189.